Indian Journal of Pure & Applied Physics
Vol. 62, April 2024, pp. 267-273
DOI: 10.56042/ijpap.v62i4.7792

# On-Orbit Response Analysis of Silicon Photodetectors in 4-Pi Sun Sensor of Aditya-L1 Mission

Sirisha J*, Bhavana D**, Amit Maji, Ishan R Gunjal, Sumesh M A & S P Karanth
Laboratory for Electro-Optics Systems, Indian Space Research Organization, Bengaluru 560 094, India

*Received 4 January 2024; accepted 5 February 2024*

Silicon photodetectors indigenously developed by Laboratory for Electro-Optics Systems (LEOS) have been used in 4-pi sun sensors (4piSS) for space craft attitude determination. A performance analysis of these detectors during their latest flight in the Aditya-L1 mission was carried out, wherein an unprecedented fall in sensor output was observed during the first seven days of flight. The possibility of variation in sensor output due to effects of ionizing radiation in the inner Van Allen belts during orbit raising is explored. The radiation environment encountered by the spacecraft during different stages of orbit raising is studied and it is seen that the spacecraft orbit was completely inside the high intensity radiation zone during the first seven days. Moreover, stabilization of the sensor output coincides with the third orbit-raising maneuver, during which the spacecraft orbit was moved outside the high intensity region of the radiation belt. The cumulative proton fluence experienced by the satellite during the initial stages was computed to be $2.6\times10^{11}$ $cm^{-2}$. This matches well with the proton fluence required to cause the observed variation in photo response, as estimated using data from previous irradiation lab experiments conducted on these photodetectors.

**Keywords**: Silicon photodetectors; 4piSS; Ionizing radiation; Aditya-L1

## 1 Introduction

Silicon (Si) photodetectors are most sought after optoelectronic detectors in aerospace, defence, industrial and satellite systems[1]. Silicon photodetectors remain integral components in precision analogue and digital sun sensors[1] for spacecraft's attitude determination and control system. They enable accurate determination of a satellite's orientation relative to the Sun, facilitating solar panel orientation for optimal power generation, aiding attitude control systems for manoeuvring and also play a role in fail safe recovery processes. Silicon photodetectors, with their reliability, rapid response times, and ability to operate across a broad spectrum[1,2] (400-1100 nm) remain integral components in sun sensor systems of Low Earth Orbit (LEO) and Geo Stationary Orbit (GEO) spacecrafts.

Due to the requirement of a large coverage of the field of view (FOV) and accuracy, multiple Sun sensors are mounted in different locations of satellites. In general, GEO satellites deploy eight Coarse Analogue Sun Sensors (CASS) for larger FOV coverage, four Solar Panel Sun sensor (SPSS) for solar panel tracking and two Digital Sun Sensors (DSS) or Active Pixel Sun Sensors (APSS) for high pointing accuracy. For LEO missions, four 4-pi sun sensors optical heads are mounted to cover $4\pi$ steradian FOV and four SPSS for solar panel tracking to the Sun. Hence, these space grade silicon photodetectors are required in large numbers, for instance, fifty numbers per satellite which amounts to an import cost of USD 50,000. Considering increased spacecraft launches per year and the associated huge foreign exchange involved for Si photodetectors alone for sun sensors, Laboratory for Electro-Optics Systems (LEOS) has successfully designed, developed and qualified Si photodetectors for space applications. More than 6000 LEOS-made space-grade Si are flown in several LEO, GEO and interplanetary missions from the year 2010 till date[3]. These include 5 mm × 5 mm Si photodetectors for 4-pi sun sensors and 5 mm × 17 mm photodetectors for Coarse Analogue Sun Sensor (CASS) and Solar Panel Sun Sensors (SPSS).

The 4-pi Sun Sensors are used for initial Sun acquisition after Injection to orbit, safe mode operation of satellites, and absolute attitude determination in conjunction with magnetometer data. These 4-pi Sun Sensors, being an indispensable element in spacecraft attitude determination, have been flown on all the LEO spacecraft launched by

*Corresponding author:
(E-mail: sirisha_j@leos.gov.in; bhavanad@leos.gov.in)

ISRO including recent missions like RISAT-1A[3], Oceansat-3[3], Aditya-L1[3] and XPoSat[3]. Due to harsh space environment and radiation effects, 4piSS Si photodetectors response degradation is observed to be around 6-7% in first year of launch and overall 15-17% in full life of satellites (5 years) as per onboard data obtained from all the ISRO's remote sensing low earth orbit spacecrafts.

This paper covers the performance of silicon photodetectors used in 4-pi sun sensors on board Aditya-L1, including certain new, unusual observations. Aditya-L1 is the first Indian space-based mission to study the Sun. Post launch, the spacecraft was placed in a Low Earth Orbit. Subsequently the orbit was made more elliptical through a series of earth-bound manoeuvres (EBN#1, EBN #2, EBN #3, and EBN #4) and it was finally launched towards the Lagrange Point (L1) by Trans Lagrangian Insertion (TLI).

Section 2 details the fabrication of the Si photodetectors, whereas their onboard performance in Aditya-L1 is analysed in Section 3. The conclusions are presented in Section 4.

## 2 Fabrication of Si photodetectors

The indigenously developed silicon (Si) photo detectors used in 4-pi sun sensors possess an n+/p structure and the cross section of the device is as shown in Fig. 1. The top n+ layer results from phosphorous ion diffusion into a 300 μm thick monocrystalline p-Si <100> wafer with a resistivity of 10 Ω.cm. This establishes a shallow n+/p junction (0.5 μm depth) producing a 35 mA/cm$^2$ short-circuit current under AM0 condition[1] (The spectrum above the Earth's atmosphere is referred to as AM0, that has integrated optical power of 1350 W/m$^2$). The specifications of the Si photo-detectors at room temperature (23±3°C) are described in Table 1.

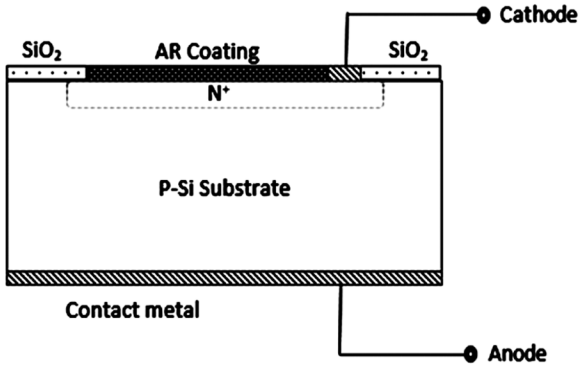


Fig. 1 — Cross section of the n+/p Si photodetectors.

The phosphorous ion diffused region defines the photodiode active area of 5 mm × 5 mm, which is surrounded by a 1 μm thick thermally grown silicon dioxide for passivation. A tri-layer metallic coating consisting of titanium (Ti), palladium (Pd) and silver (Ag) is deposited sequentially on an identified bus bar area, within the N+ diffusion region, as well as on the entire rear side area of the device, using ion beam sputtering technique[1].Titanium (Ti) coating thickness of 70 nm is used to ensure adhesion of metallization coating, and a barrier layer of palladium (Pd) coating of 30 nm thickness prevents diffusion of highly mobile Ag atoms and galvanic corrosion. Additionally, Silver (Ag) of thickness 1800 nm is deposited to take the solder contacts using silver foil.

Substance-2 ($PrTiO_3$ of Merck Brand) is deposited as an anti-reflection coating. It provides refractive index matching with Si substrate reduces the surface reflectance to less than 5% in the wavelength of interest (400 to 900 nm) that enhances visible optical throughput into detector in order to obtain better external quantum efficiency. Fig. 2 illustrates soldered contacts on the front bus bar (cathode) and entire rear side (anode), utilizing 99.99% pure silver foil. To assess the space worthiness of Si photo-detectors and to qualify them for space applications,

Table 1 — Specifications of Si photodetectors.

| Sl. No. | Parameter | Specifications |
|---|---|---|
| 1. | Type of Detector | PV (Photovoltaic) |
| 2. | Spectral Range | 400 - 1100 nm |
| 3. | Responsivity | ≥ 0.57 A/W (740-950 nm) |
| 4. | Short circuit current | ≥ 7 mA at AM0 |
| 5. | Dark current | ≤ 10 nA at –2V (at 23±3 °C) |
| 6. | Reverse breakdown | < 1 μA at -5V |
| 7. | Junction capacitance | < 5 nF at -2V |
| 8. | Series resistance | 1-5 Ω |
| 9. | Shunt resistance | ≥30 MΩ |

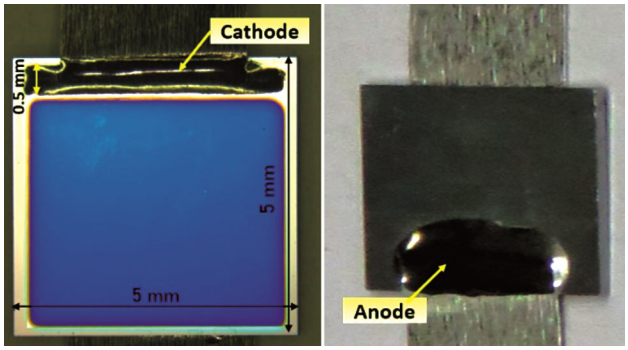


Fig. 2 — Front and rear side of 5 mm × 5 mm silicon photodetectors.

rigorous space qualification tests were carried out as per the test and evaluation matrix specified in[1].

## 3 Performance in Aditya-L1

### 3.1 4-pi Sun Sensor Description

The 4piSS optical head consists of 5mm×5mm Si-photodetectors to meet the signal to noise ratio (SNR) and sensor accuracy. In a 4-pi Sun Sensor optical head, two photodetectors named as main and redundant are mounted on three faces of cube as shown in Fig. 3(a). Four sensors are mounted on the spacecraft to ensure a total angular coverage of 4π steradians. The detectors are operated in photovoltaic mode with no electrical bias. The 4piSS is a robust sun sensor, working on the principle of cosine law. When Sunlight falls on detector in different incident angles, the photodetector generates current as per cosine law principle as shown in Fig. 3(b). The photocurrent (~ 7 mA) is converted to voltage using current to voltage converter (I-V) with a gain of 570 ohms. This voltage is logged using an Analog to Digital Converter (ADC) module and telemetered to ground.

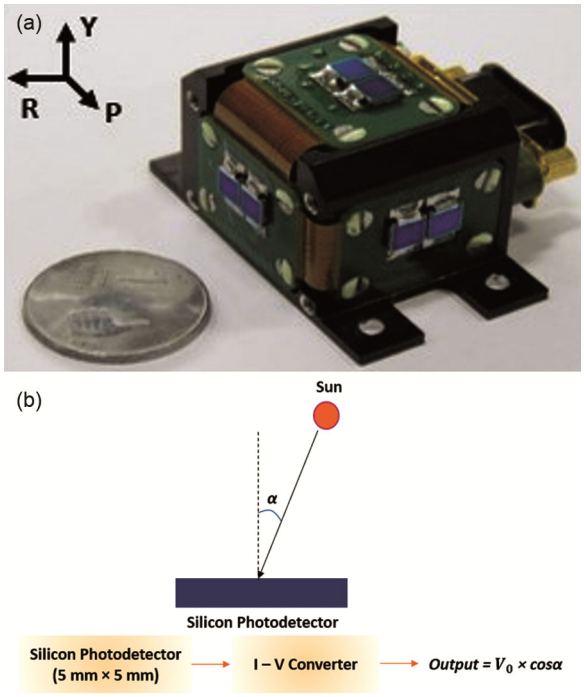


Fig. 3 — (a) –Photograph of 4piSS optical head consisting of main and redundant Si photodetectors on three faces (Y-Yaw, R-Roll, P-Pitch) of sensor head.

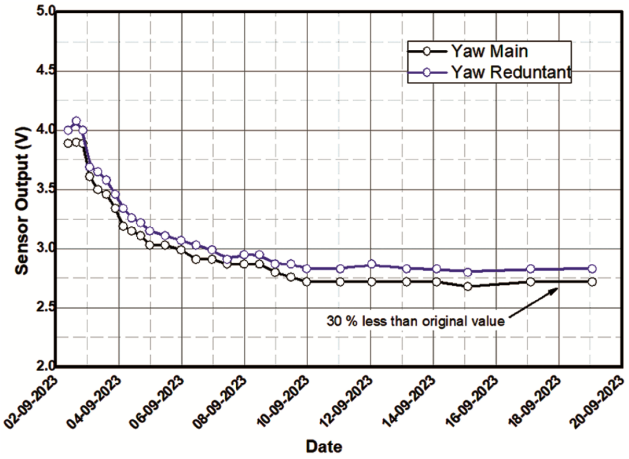


Fig. 4 — Onboard data showing Yaw Sun Sensor output.

### 3.2 Observations

Aditya-L1 was launched on 2nd September, 2023 and Yaw axis of satellite is always facing the Sun for payload operation. Yaw main and Yaw redundant are two photodetectors mounted normal to the Yaw axis of the space craft facing the sun. Both, Yaw main and Yaw redundant are expected to show output current within 5% variability. After the launch of the satellite, 4piSS Yaw cells (Si photo detectors) output voltage gradually reduced from 4 V to 2.8 V as shown in Fig. 4. The photodetector response degradation was observed for both main and redundant cells simultaneously. Although output data is sampled for every 16 msec, Fig. 4 represents only the average value over daily time periods. The degradation of photodetectors on other axes (Roll and Pitch) could not be verified due to the satellite's orientation and the sun rays never fall on roll and pitch faces of satellite. The reduction in sensor output was observed only during the first 7 days, after which the sensor output stabilized at 70 % of the original value.

### 3.3 Radiation Environment Encountered by Aditya-L1

The radiation environment encountered by satellites in altitudes higher than LEO is dominated by high energy protons and electrons trapped in the Van Allen belts. Protons in the range 5 – 15 MeV are the most deleterious for solar cell arrays[4]. The fluxes observed by the satellite on orbit depend on the orbital inclination and altitude. The greatest inclination dependencies occur in the range from 0° to 30° [5]. The Aditya L1 orbit has an inclination of 19.2°, and the spacecraft passes through the high radiation zone of the belt two times in each orbit as shown in Fig. 5.

Detailed trajectory of the Aditya L1 specific to the radiation belt transit is given in Figs. 6 & 7. The proton flux model AP8MIN is used for arriving at the fluence values[6]. It is seen that for a threshold energy

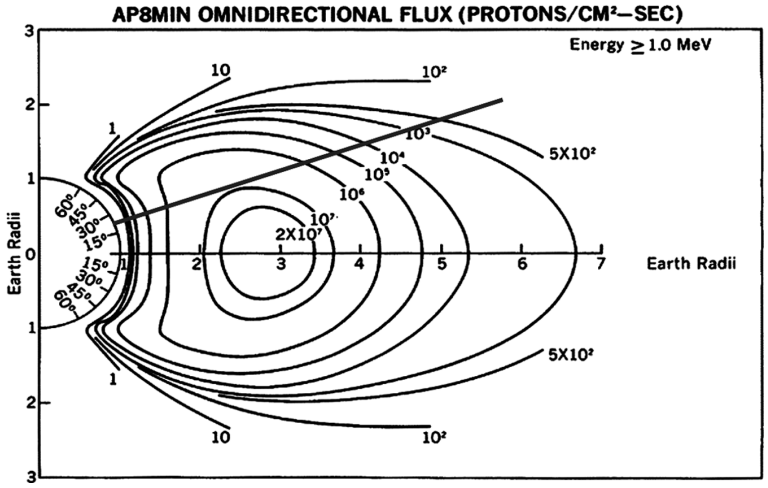


Fig. 5 — Constant Intensity Contour of Omnidirectional Proton Flux Density for Energy ≥1MeV[6]. The blue line shows an inclination of 19.2° that corresponds to Aditya L1 orbit.

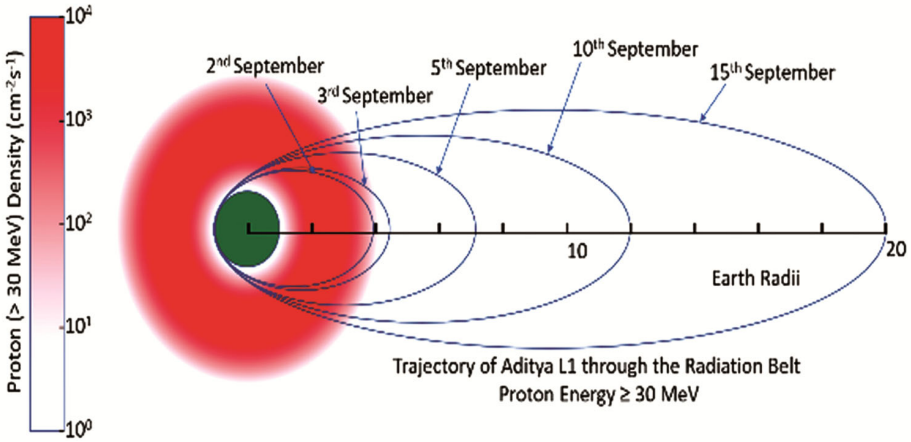


Fig. 6 — Trajectory of Aditya L1 showing its multiple passes through the high energy radiation zone (≥ 30 MeV) before Trans Lagrangian Insertion (TLI).

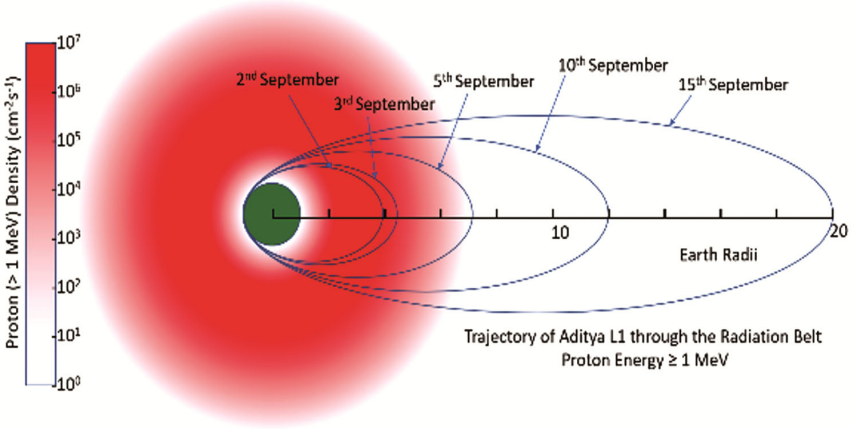


Fig. 7 — Trajectory of Aditya L1 showing its multiple passes through the high intensity radiation zone (≥ $10^7$ Particles $cm^{-2}s^{-1}$) before the TLI.

Table 2 — Mission stages of the Aditya L1 spacecraft

| Stage | Date, Time (IST) | Periapsis (km) | Apoapsis (km) |
|---|---|---|---|
| Launch | 02/09/2023, 12:54 | 235 | 19,500 |
| EBN#1 | 03/09/2023, 11:40 | 245 | 22,459 |
| EBN#2 | 05/09/2023, 3:00 | 282 | 40,225 |
| EBN#3 | 10/09/2023, 2:30 | 296 | 71,767 |
| EBN#4 | 15/09/2023, 2:15 | 256 | 1,21,973 |
| TLI | 19/09/2023, 2:00 | - | - |

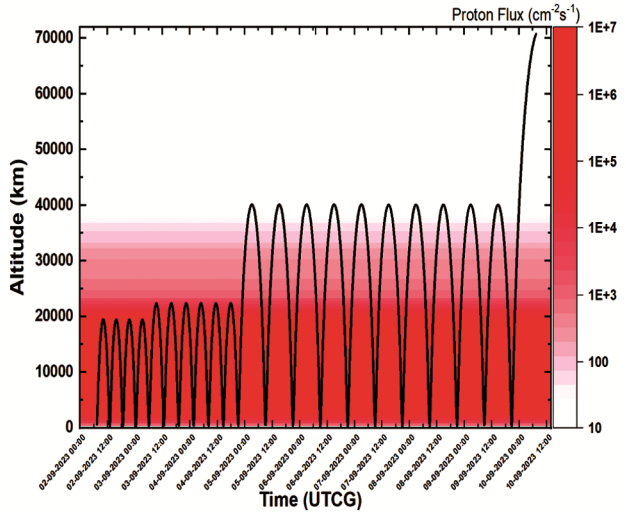


Fig. 8 — Altitude of the Aditya L1 during in the initial stages of manoeuvres showing its multiple passes through the high energy radiation zone (≥ 30 MeV) before TLI.

of 30 MeV, high proton flux is observed in the inner belt region that extends from 1.1 to 3 earth radii with a peak flux value of > $10^4$ $cm^{-2}s^{-1}$ at 2.5 earth radii.

However, the proton fluxes are much more intense for lower energy threshold (> 1 MeV) for which the flux values reach as high as $10^7$ $cm^{-2}s^{-1}$ at about 3 earth radii. With an inclination of 19.2°, the spacecraft passes through the high energy radiation zone multiple times during the orbit. The integrated proton fluence will be a function of the duration for which the spacecraft has been in this radiation region. Table 2 gives the details of the mission stages.

On the day of launch i.e. 2nd Sept, 2023, the spacecraft was put into an elliptical orbit with Periapsis: 235 km and Apoapsis: 19500 km. While in this orbit, the spacecraft was completely inside the high intensity radiation zone for more than 22 hrs. On 3rd September, the first Earth-bound manoeuvre (EBN#1) was executed to raise the orbit to 22,459 km and on 5th September, the orbit was raised further to 40,255 km (EBN#2). Therefore, the spacecraft was residing completely inside the high intensity radiation belt zone with an average proton flux of ~$10^6$ $cm^{-2}s^{-1}$ till 5th September as shown in Fig. 8. During this period of three days, the silicon photo detectors would have experienced a cumulative fluence of $2.6\times10^{11}$ $cm^{-2}$.

EBN#3 was executed on 10th September, in which the orbit was raised to 71,767 km. In this orbit, the space craft spends less time in the high radiation zone and remains mostly away from radiation belt. Hence, subsequent to EBN#3, the spacecraft encountered a lower radiation dosage, and this corresponds to a stabilization in the sensor output as evident from Fig. 4. Further no reduction in sensor output was observed.

### 3.4 Performance Analysis and Inferences

As the time period of performance degradation corresponds to the orbit raising stage of the satellite, exposure of the uncovered silicon photodetectors to ionizing radiation from inner Van Allen radiation belt could be a key reason for the reduction in photocurrent.

The process of orbit raising through the Van Allen radiation belts can have a detrimental effect on the performance of photodetectors[7]. The performance degradation can be attributed to lattice displacement and ionization damage[8] in silicon photodetectors on their exposure to large fluences of high-energy photons trapped in the radiation belts.

The effects of high energy radiation on the photo response and dark current density of the indigenously developed silicon photodetectors have been thoroughly studied by experimental methods. This includes investigations in terms of Total Ionizing Dose[8] (TID), Swift Heavy Ion irradiation[9] as well as high energy proton and electron fluence relevant to GEO and LEO bound spacecrafts. The results of experiments carried out to study the high energy radiation exposure effects on three different photodetectors and their performance are compiled in Table 3.

The detector performance is evaluated under AM0 condition using a sun simulator (Make: Holmarc Opto-mechatronics Ltd) by measuring the photo response pre and post irradiation. Xenon Arc lamp serving as a sun simulator is calibrated for AM0 condition using standard silicon detector (Make: Hamamatsu). The current output of the detector under test (DUT) is measured through a Digital Multimeter (Make: Keithley) under AM0 condition pre and post

Table 3 — Effect of high energy ionizing radiation on three different silicon photodetectors: Experimental results.

| Device | Type of Radiation | Fluence ($cm^{-2}$) | Observation |
|---|---|---|---|
| Silicon Photo Detector[1] | Electron (8 MeV) | $1\times10^{14}$ | 17% degradation in photoresponse |
| Silicon Photo Detector[1] | Electron (1 MeV) | $5\times10^{14}$ | 15% degradation in photoresponse |
| Dual Axes Micro Sun Sensor[10] | Proton (21.5 MeV) | $8.7\times10^{10}$ | 19.5% degradation in photoresponse |

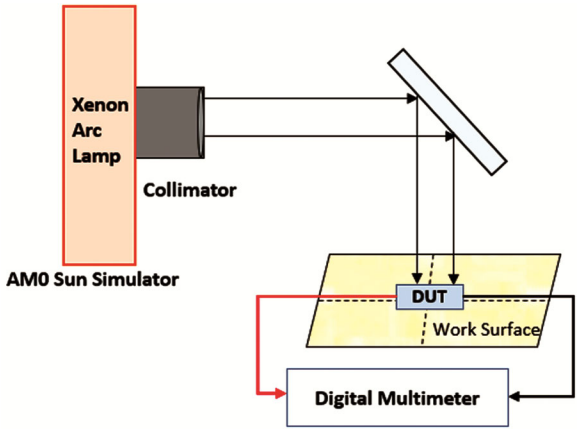


Fig. 9 — Block Schematic for measuring photo response of Si photodetector under AM0 condition.

irradiation as shown in the Fig. 9. The short circuit current obtained is normalised with circuit current density. The short circuit current densities of these detectors, both pre ($J_0$) and post ($J$) irradiation, were evaluated at same temperature *i.e.* at room temperature.

As the inner radiation belt is dominated by protons, the performance degradation of 19.5% experienced by Dual Axes Sun Sensor after exposure to high energy protons is considered to estimate the radiation damage coefficient.

The radiation damage coefficient is related to the diffusion length of a photodetector as follows[11]:

$$\left(\frac{1}{L}\right)^2 = \left(\frac{1}{L_0}\right)^2 + K\emptyset \qquad \ldots(1)$$

Where, $L_0$ and $L$ are the diffusion lengths of un-irradiated and irradiated devices respectively,$\emptyset$ is the proton fluence, and $K$ is the diffusion length damage coefficient for proton irradiation. As the detector current density is directly proportional to the diffusion length, Eq. 1 can be rewritten as

$$\left(\frac{J_0}{J}\right)^2 = 1 + {L_0}^2 K\emptyset \qquad \ldots(2)$$

where, $J_0$ and $J$ are the short circuit current densities of un-irradiated and irradiated devices respectively.

In the case of the Dual Axes Sun Sensor, the short circuit current densities before and after proton irradiation are 15.08 mA/cm$^2$ and 12.14 mA/cm$^2$ respectively for a total fluence of $8.7 \times 10^{10}$ cm$^{-2}$. The diffusion length ($L_0$) is considered to be 100 µm[1,12]. Thus, damage coefficient for protons, $K$ has been evaluated using Equation 2 to be $6.2 \times 10^{-4}$.

From Fig. 4, the current output for silicon photodetector drops from 4 V to 2.8 V. Proton fluence that the device could have encountered onboard is estimated using Equation 1 to be $1.68\times 10^{11}$ cm$^{-2}$. This value is in agreement with the proton fluence encountered by the spacecraft during the initial orbit-raising stage as calculated in Section 3.3.

## 4 Conclusion

4-pi Sun Sensors using indigenous silicon photodetectors were deployed in Aditya-L1 spacecraft. During the initial phase of the flight, the sensor output gradually reduced by about 30 % of the initial value in 7 days. The sensor output was stable later on and no further reduction was observed. The reason for this sensor output reduction was analysed based on the high energy trapped proton flux prevailing in the radiation belt zones. It is evident that, till the EBN#3 on 10$^{th}$ September, 2023, the spacecraft was completely inside the high intensity radiation zone, causing a cumulative proton fluence of $2.6\times10^{11}$ cm$^{-2}$. After EBN#3, the spacecraft spent a shorter duration in the radiation zone and the sensor output stabilized from then on. From the proton irradiation lab experimental studies carried out on the indigenous silicon photodetectors, the proton fluence corresponding to the observed variation in the photo current response was calculated to be $1.68\times10^{11}$ cm$^{-2}$. This is in close agreement with the estimated fluence encountered by the spacecraft during the first three days of orbit raising. Hence, it is understood that the variation in the 4-pi sensor output is due to the exposure of the silicon photodetector to the high energy protons trapped in the radiation zone through which the spacecraft passed during the initial stages of the orbit raising. Further, research towards improved radiation resistant semiconductor detector development for sun sensors are being pursued, mainly on tandem a-SiC/a-Si photodetectors.

**Acknowledgments**

The authors are thankful to Dr. Sriram K V, Director, LEOS/ISRO for providing encouragement and resources for carrying out the work presented in the paper.

Authors express their gratitude to Microtron Center, Mangalore University and Tata Institute of Fundamental Research (TFIR), Mumbai for providing their facilities to carry out electron and proton irradiation respectively.

**References**

1 Karanth S P, Sharma S V K & Nagendra C L, *J Spacecraft Technol*, 16 (2016) 41.

2 Ding N, Wu Y, Xu W, *et al*., *Light: Sci Appl*, (2022).

3 *https://www.isro.gov.in/Satellites.html*

4 Vette J I, Trapped Radiation Environment Model Program, Tech Rep, NSSDC/WDC-A-R & S 91-29, The NASA/ National Space Science Data Center, (1991).

5 Märki A, *Int J Astrophys Space Sci*, 8 (2020) 16.

6 Sawyer D M & Vette J I, AP8 Trapped Proton Environment for Solar Maximum and Solar Minimum, Tech Rep, NSSDC WDC-A-R&S 76-06, NASAGSFC, The NASA/National Space Science Data Center, (1976).

7 Messenger S R, Wong F, Hoang B, *et al.*, *IEEE Trans Nucl Sci*, 61 (2014) 3348.

8 Kumar V M, Kumar S, Cheng C, *et al.*, *ECS J Sol-State Sci Technol*, 6 (2017) 132.

9 Kumar V M, Verma S, Asokan K, *et al.*, *ECS J Sol-State Sci Technol*, 5 (2016) 384.

10 Bhavana D, Sirisha J, Sumesh M A, *et al.*, *Indian J Pure Appl Phys*, 61 (2023) 85.

11 Tada Y, Solar cell Radiation Handbook (JPL publication), 3rd Edn, (1989) 82.

12 Karanth S P, Shobha V & Sumesh M A, *et al*., *J Small Satell*, 6 (2017) 581.